also not as high and the associated kinetic energy release (3.2 eV) is larger.

Ar_2^{2+} Dication. The calculated stability of the argon dimer dication **9**, like that of the hydrogen fluoride dimer dication **4**, is sensitive to the introduction of electron correlation into the calculations. At the Hartree-Fock level, **9** is predicted to be unbound, but at the UMP2 level, a barrier of 65 kJ mol^{-1} impedes its fragmentation. However, more sophisticated correlation treatments reduce this barrier until, at the level of fourth-order perturbation theory (RMP4), it disappears altogether. However, at this level, it appears that the potential curve is rather flat for $2 < r < 3$ Å, and this plateau may be detectable in collision experiments. The simple ACDCP model[10] for the fragmentation of a diatomic dication predicts that the transition-structure bond length in the case of Ar_2^{2+} is 2.24 Å, which is similar to that (2.159 Å) of the UMP2/6-31G(d) structure **17**.

Concluding Remarks

Many of the important results of this paper are summarized in Table VI, and it is useful to note some of the features of dicationic structure and stability that are revealed in this table.

(1) The dimer dications (A_2^{2+}) are more tightly bound than corresponding (hemibonded) monocations ($A_2^{\bullet+}$) in the sense of exhibiting shorter equilibrium A-A bond lengths, but the dissociation barriers are generally smaller (and in some cases close to zero) for the dications.

(2) Transition-structure bond lengths and the associated barriers for the symmetric fragmentations and deprotonations of the dimer dications $H_nXXH_n^{2+}$ are largest when X is a group V element, and both quantities decrease from left to right across the periodic table. This is in accord with the qualitative predictions of the ACDCP model (vide supra) but contrasts with the pattern of hemibond strengths in the related $H_nXXH_n^{\bullet+}$ systems,[2] which are greatest when X is from group VII.

(3) The hydrazinium and diphosphinium dications (**2** and **6**, respectively) should form very stable salts. Three of the remaining dimer dications ($H_2OOH_2^{2+}$, $H_2SSH_2^{2+}$, and $HClClH^{2+}$) may be experimentally observable under certain (nonequilibrium, low-temperature, or short-time-scale) conditions. The other dimer dications ($HFFH^{2+}$, Ne_2^{2+}, and Ar_2^{2+}) appear to be unstable.

(4) The equilibrium structures of the dimer dications are comparable to those in their isoelectronic, isostructural, neutral analogues. For example, the geometries of He_2^{2+} (**1**) and $H_3NNH_3^{2+}$ (**2**) are very similar to those of the hydrogen and ethane molecules, respectively.

(5) The value of the Δ parameter for a dicationic fragmentation is a very useful indicator of the dissociation behavior. Thus, (a) a small Δ value (less than $\sim$2-3 eV) indicates that the associated transition structure will be late and, in such cases, Δ constitutes a reliable measure of the consequent kinetic energy release; (b) for fragmentations with larger Δ values, the transition structures occur earlier along the reaction coordinate, and the resulting kinetic energy releases are larger, though bounded above by Δ; and (c) if the Δ value for a fragmentation is large (greater than $\sim$15 eV), the barrier inhibiting the fragmentation is likely to be small or nonexistent. A notable exception is the extraordinary He_2^{2+} dication **1**.

Acknowledgment. We gratefully acknowledge a generous allocation of time on the Fujitsu FACOM VP-100 of the Australian National University Supercomputer Facility.

Supplementary Material Available: Calculated total energies, zero-point vibrational energies, and $\langle S^2 \rangle$ values of the dimeric dications, their deprotonated and dehydrogenated forms, and relevant transition structures (Table VII) and of fragment neutrals, monocations, and dications (Table VIII) (4 pages). Ordering information is given on any current masthead page.

A Theoretical Investigation of the Primary Dissociation Paths of Ethynylsilane

J. J. W. McDouall, H. B. Schlegel, and J. S. Francisco*

Contribution from the Department of Chemistry, Wayne State University, Detroit, Michigan 48202. *Received July 5, 1988*

Abstract: Various mechanisms leading to the dissociation of ethynylsilane have been investigated by ab initio molecular orbital methods. Geometries corresponding to the reactant, transition states, and products have all been optimized at the HF/3-21G and HF/6-31G* levels of theory. Heats of reaction and barrier heights have been obtained at the MP4SDTQ/6-31G* level. Zero-point energy corrections and harmonic vibrational frequencies have been computed at the HF/3-21G level. These results have been used to calculate unimolecular dissociation rate constants by RRKM theory. This information is then used to reexamine the mechanisms of dissociation for ethynylsilane from previous experimental shock-tube and stirred-flow studies.

It has become generally accepted that the predominant dissociation process in alkyl-, alkenyl-, and arylsilanes is the formation of hydrogen via

$$RSiH_3 \rightarrow RSiH + H_2 \quad (1)$$

with alkanes (or alkenes) formed from minor channels for primary dissociation pathways

$$RSiH_3 \rightarrow RH + SiH_2 \quad (2)$$

or secondary reaction from the substituted silylene formed in reaction 1.

$$RSiH \rightarrow R'H + SiH_2 \quad (3)$$

It is the minor and secondary channels that are responsible for the production of SiH_2, an intermediate acknowledged to be important in the formation of amorphous silicon thin films. Results from numerous shock-tube and photodissociation studies[1-10] of

(1) Ring, M. A.; O'Neal, H. E.; Rickburn, S. F.; Sawrey, B. A. *Organometallics* **1983**, *2*, 1891.
(2) Sawrey, B. A.; O'Neal, H. E.; Ring, M. A.; Coffey, D., Jr. *Int. J. Chem. Kinet.* **1984**, *16*, 31.
(3) Sawrey, B. A.; O'Neal, H. E.; Ring, M. A.; Coffey, D., Jr. *Int. J. Chem. Kinet.* **1984**, *16*, 801.
(4) Rickburn, S. F.; Ring, M. A.; O'Neal, H. E. *Int. J. Chem. Kinet.* **1984**, *16*, 1371.

0002-7863/89/1511-4622$01.50/0

a variety of organosilanes support the general claim that reaction 1 is the predominant primary dissociation process. In a series of ab initio molecular orbital studies, we have examined the relative importance of primary dissociation pathways for the simplest alkyl- and alkenylsilanes.[11,12]

Both experimental and theoretical studies support the claim that 1,1 H_2 elimination predominates the primary dissociation process of small alkylsilanes such as methylsilane[5-7,13,14] and ethylsilane.[1,4,11]

$$CH_3SiH_3 \rightarrow CH_3SiH + H_2 \quad (4)$$

$$CH_3CH_2SiH_3 \rightarrow CH_3CH_2SiH + H_2 \quad (5)$$

Studies on vinylsilane,[1,9,12] the simplest alkenylsilane, reveal that the predominant dissociation leads to the formation of hydrogen via

$$CH_2{=}CHSiH_3 \rightarrow CH_2{=}CHSiH + H_2 \quad (6)$$

However, theoretical studies[12] have predicted 1,2 silyl shifts to be competitive with reaction 6. The simplest alkynylsilane is ethynylsilane; its major dissociation product is acetylene as shown from shock-tube and stirred-flow studies.[15,16] The dominant mechanism of dissociation has been suggested to involve 1,1 hydrogen elimination.

$$HC{\equiv}CSiH_3 \rightarrow HC{\equiv}CSiH + H_2 \quad (7)$$

In this work we have investigated primary reaction pathways for ethynylsilane to determine if the 1,1 hydrogen elimination is also predominant over all other processes.

Computational Methods

All calculations were performed with the GAUSSIAN 86 suite of programs[17] using split-valence (3-21G)[18] and polarized (6-31G*)[19] basis sets. All equilibrium and transition-state geometries were fully optimized at the Hartree–Fock level using analytical gradient methods.[20] The effects of electron correlation were estimated by Møller–Plesset perturbation theory to fourth order[21] (including all single, double, triple, and quadrupole excitations, frozen-core approximation). Harmonic vibrational frequencies were obtained from analytical second derivatives[22] calculated

Table I. Optimized Geometries of Reactant, Transition States, and Products

	$HCCSiH_3$[a]		[CCH(SiH$_3$)]‡				:CCH(SiH$_3$)[c]		[HCCSiH + H$_2$]‡[a]		HCCH + :SiH$_2$[a]		HCCSiH + H$_2$[a]		[C$_2$H$_2$ + SiH$_2$]‡[a]		C≡CSiH$_3$[a]		HC≡C + SiH$_3$[a]		HCCSiH$_2$	
			1,2 silyl[b]		1,2 hydrogen[c]																	
	3-21G	6-31G*	3-21G	6-31G*	3-21G	6-31G*	3-21G	6-31G*	3-21G	6-31G*	3-21G	6-31G*	3-21G	6-31G*	3-21G	6-31G*	3-21G	6-31G*	3-21G	6-31G*	3-21G	6-31G*
R(H_2H_3)[d]									1.121	1.086			0.735	0.730								
R(C_1C_2)	1.195	1.194	1.248	1.254	1.252	1.244	1.285	1.284	1.195	1.194	1.188	1.185	1.200	1.200	1.199	1.199	1.233	1.228	1.224	1.215	1.205	1.202
R(C_1H_4)	1.052	1.058	1.056	1.066	1.225	1.169			1.052	1.058	1.051	1.057	1.052	1.058	1.052	1.059			1.053	1.058	1.052	1.058
R(SiC_2)	1.861	1.838	2.172	2.307	1.879	1.861	1.914	1.890	1.854	1.830			1.882	1.848	2.100	2.075	1.863	1.839			1.844	1.821
R(SiH_1)	1.483	1.472	1.475	1.467	1.480	1.469	1.481	1.470	1.479	1.468			1.528	1.506	1.634	1.618	1.483	1.472	1.487	1.476	1.483	1.472
R(SiH_2)	1.483	1.472	1.475	1.467	1.481	1.469	1.483	1.472	1.533	1.516	1.531	1.509			1.487	1.476	1.483	1.472	1.487	1.476	1.483	1.472
R(SiH_3)	1.483	1.472	1.486	1.475	1.481	1.469	1.483	1.472	1.688	1.644	1.531	1.509			1.487	1.476	1.483	1.472	1.487	1.476		
R(SiC_1)			2.163	1.985																		
R(C_2H_4)					1.434	1.469	1.076	1.078							1.332	1.272						
R(C_2H_1)																						
H_1SiH_2[e]	109.49	109.44	108.65	110.69	110.92	111.09	109.89	109.98	111.97	109.86									111.66	108.02	112.54	111.61
H_2SiH_3											93.80	93.32										
H_1SiC_2	109.45	109.51	100.94	97.84	105.79	105.39	109.72	109.52	146.18	146.26			94.88	95.30							111.48	110.02
H_2SiC_2	109.45	109.51	100.94	97.84	109.64	109.68	108.91	109.03	112.27	111.87					93.96	91.99	109.27	109.31			111.48	110.02
H_3SiC_2	109.45	109.51	125.88	130.88	109.64	109.68	108.91	109.03	93.65	93.85					93.96	91.99	109.27	109.31				
C_1C_2Si	180.00	180.00	72.87	59.29	174.95	178.13	116.65	114.11	177.06	174.60			177.28	174.88	172.33	179.88						
$H_4C_1C_2$	180.00	180.00	162.92	152.84	53.76	50.21			179.88	179.76			179.86	179.39	179.74	182.22						
$H_4C_2C_1$							123.85	123.86														

[a] See Figure 1a for atom numbering. [b] See Figure 1d for atom numbering. [c] See Figure 1e for atom numbering. [d] Bond lengths in angstroms. [e] Bond angles in degrees.

(5) Davidson, I. M. T.; Ring, M. A. *J. Chem. Soc., Faraday Trans. 1* **1980**, *76*, 1520.
(6) Neudorfyl, P. S.; Strausz, O. P. *J. Phys. Chem.* **1978**, *82*, 241.
(7) Sawrey, B. A.; O'Neal, H. E.; Ring, M. A.; Coffey, D., Jr. *Int. J. Chem. Kinet.* **1984**, *16*, 23.
(8) Dzarnoski, J.; O'Neal, H. E.; Ring, M. A. *J. Am. Chem. Soc.* **1981**, *103*, 5740.
(9) Rickburn, S. F.; Ring, M. A.; O'Neal, H. E.; Coffey, D., Jr. *Int. J. Chem. Kinet.* **1984**, *16*, 289.
(10) Baggot, J. E.; Frey, H. M.; Lightfoot, P. D.; Walsh, R. *Chem. Phys. Lett.* **1986**, *125*, 22.
(11) Francisco, J. S.; Schlegel, H. B. *J. Chem. Phys.* **1988**, *88*, 3736.
(12) Francisco, J. S., to be published in *J. Am. Chem. Soc.*
(13) Gordon, M. S.; Truong, T. N. *Chem. Phys. Lett.* **1987**, *142*, 110.
(14) Neudorfl, P. S.; Lown, E. M.; Safarik, I.; Jodhan, A.; Strauz, O. P. *J. Am. Chem. Soc.* **1987**, *109*, 5780.
(15) Rogers, D. S.; Ring, M. A.; O'Neal, H. E. *Organometallics* **1986**, *5*, 1521.
(16) Ring, M. A.; O'Neal, H. E.; Erwin, J. W.; Rogers, D. S. *Mater. Res. Soc. Symp. Proc.* **1984**, *32*.
(17) Frisch, M. J.; Binkley, J. S.; DeFrees, D. J.; Raghavachari, K.; Schlegel, H. B.; Whiteside, R. A.; Fox, D. J.; Martin, R. L.; Fluder, E. M.; Melius, C. F.; Kahn, L. R.; Stewart, J. J. P.; Bobrowicz, F. W.; Pople, J. A. *GAUSSIAN 86*; Carnegie-Mellon Quantum Chemistry Publishing Unit: Pittsburgh, PA, 1984.
(18) Binkely, J. S.; Pople, J. A.; Hehre, W. J. *J. Am. Chem. Soc.* **1980**, *102*, 939.
(19) Gordon, M. S.; Binkely, J. S.; Pietro, W. J.; Hehre, W. J. *J. Am. Chem. Soc.* **1982**, *104*, 2797.
(20) Schlegel, H. B. *J. Comput. Chem.* **1982**, *3*, 214.
(21) Krishnan, R.; Pople, J. A. *Int. J. Quantum Chem., Quantum Chem. Symp.* **1980**, *14*, 91.
(22) Pople, J. A.; Krishnan, R.; Schlegel, H. B.; Binkely, J. S. *Int. J. Quantum Chem., Quantum Chem. Symp.* **1979**, *13*, 225.

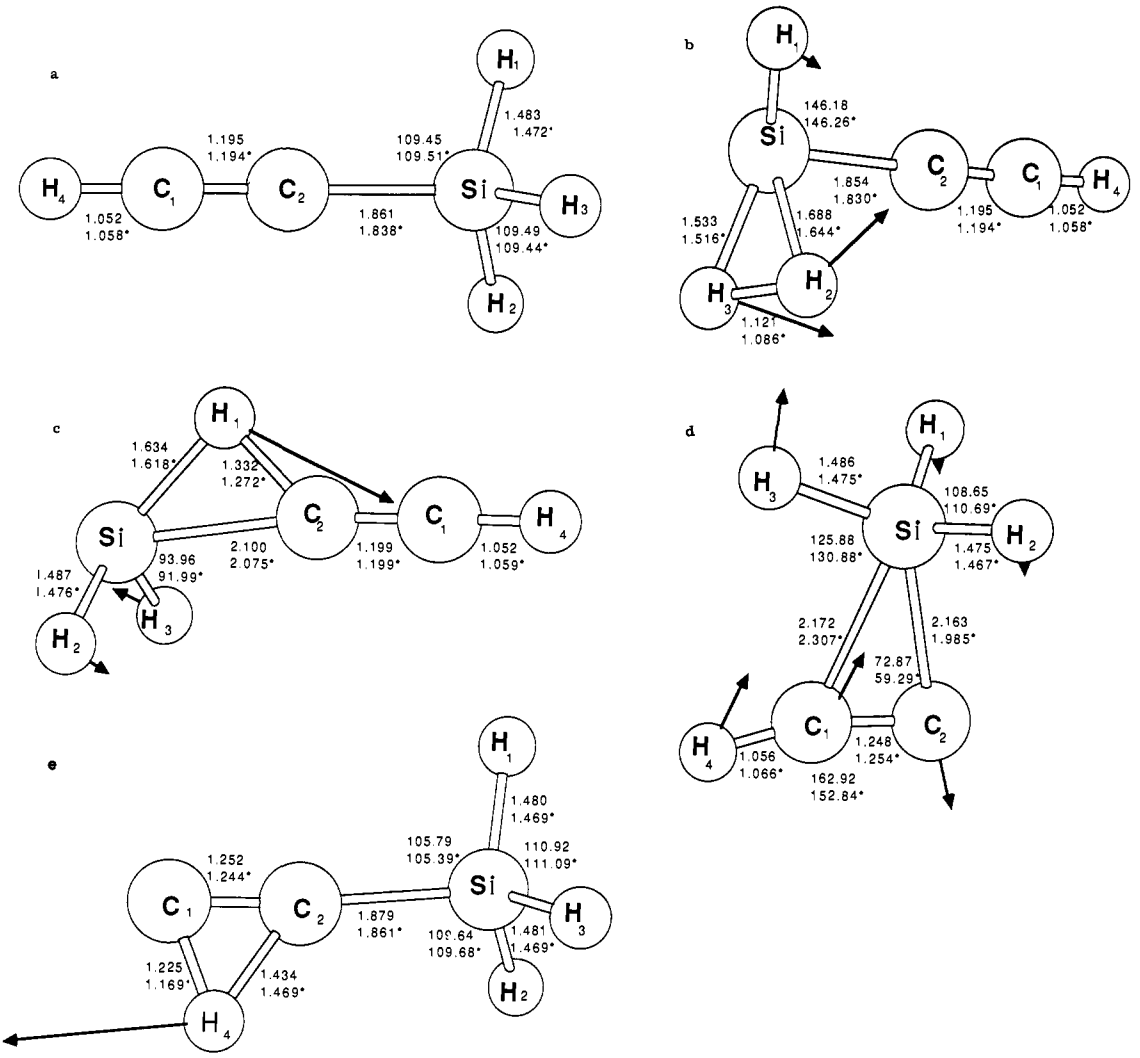

Figure 1. Reactants and transition states for the dissociation of ethynylsilane (HF/3-21G-optimized geometry, no superscript; HF/6-31G*-optimized, asterisk; see Table I for the complete list of geometrical parameters).

at the HF/3-21G//HF/3-21G level. Finally, unimolecular rate constants were obtained by RRKM theory[23] using the HF/3-21G unscaled harmonic frequencies and the MP4SDTQ/6-31G*//HF/6-31G* estimates of the reaction barrier corrected for zero-point energy.

Results and Discussion

In addition to reaction 7 mentioned above, our study of the primary dissociation pathways of ethynylsilane includes the following pathways:

$$HC{\equiv}CSiH_3 \rightarrow HC{\equiv}CSiH + H_2 \quad (7)$$

$$HC{\equiv}CSiH_3 \rightarrow C_2H_2 + SiH_2 \quad (8)$$

$$HC{\equiv}CSiH_3 \rightarrow :C{=}CH(SiH_3) \quad (9)$$

$$HC{\equiv}CSiH_3 \rightarrow CCSiH_3 + H \quad (10)$$

$$HC{\equiv}CSiH_3 \rightarrow CCH + SiH_3 \quad (11)$$

$$HC{\equiv}CSiH_3 \rightarrow HCCSiH_2 + H \quad (12)$$

The optimized geometries and transition states for reactions 7–12 are summarized in Table I, and the transition-state structures obtained for reaction 7–9 are displayed in Figure 1. The structural features for ethynylsilane calculated at the HF/6-31G* level are in good agreement with values derived from microwave data[24,25] (CC = 1.826 ± 0.003 Å, CSi = 1.207 ± 0.006 Å, and SiH = 1.455 ± 0.002 Å).

(23) Hase, W. L.; Bunker, D. L.; *QCPE* **1973**, *234*.
(24) Muenter, J. S.; Laurie, V. W. *J. Chem. Phys.* **1963**, *39*, 1181.
(25) Gerry, M. C. L.; Sugden, T. M. *Trans. Faraday Soc.* **1965**, 2091.

Table II. Vibrational Frequencies[a]

reactant: $HC{\equiv}CSiH_3$	transition structures: 1,2 silyl	$[CCH(SiH_3)]^*$ 1,2 hydrogen	$[C_2H_2 + SiH_2]^*$	$[HCCSiH + H_2]^*$
332 E	349*i* a′	1179*i* a′	1447*i*	1727*i*
655 A_1	188 a″	100 a″	303	327
742 E	501 a′	296 a″	328	366
980 E	663 a′	347 a′	489	617
1007 A_1	682 a″	625 a′	698	666
1026 E	801 a″	735 a′	818	755
2299 E	952 a′	746 a″	840	851
2310 A_1	1004 a′	988 a′	964	945
2338 A_1	1025 a′	1007 a″	976	1000
3651 A_1	1034 a″	1036 a′	981	1110
	1971 a′	2056 a′	1730	1548
	2284 a′	2311 a″	2263	2153
	2341 a′	2319 a′	2272	2319
	2346 a″	2323 a′	2282	2330
	3585 a′	2354 a′	3645	3652

[a] Harmonic vibrational frequencies in reciprocal centimeters calculated at the HF/3-21G level.

If viewed from the reverse direction, the 1,1 hydrogen elimination reaction 7 is a ethynylsilylene insertion into hydrogen. This reaction takes place via a three-centered transition state as shown in Figure 1b. As discussed above, these reactions are considered prototypical of reactions involving organosilane decompositions. The major structural features of the transition state include the approach of H_2 roughly parallel to the RSiH plane and bisecting the RSiH angle accompanied by a lengthening of the H_2 bond;

Table III. Total Energies[a]

compd	HF/3-21G	HF/6-31G*	MP2/6-31G*	MP3/6-31G*	MP4SDQ/ 6-31G*	MP4SDTQ/ 6-31G*
$HC{\equiv}CSiH_3$	-364.965 21	-366.915 28	-367.237 62	-367.258 33	-367.266 67	-367.281 00
$C_2H_2 + SiH_2$	-364.880 25	-366.817 60	-367.131 69	-367.159 19	-367.169 04	-367.181 06
$HCCSiH + H_2$	-364.894 07	-366.822 73	-367.151 12	-367.175 28	-367.185 18	-367.198 87
$CCH(SiH_3)$	-364.902 84	-366.858 59	-367.161 17	-367.191 97	-367.200 84	-367.212 99
$H + CCSiH_3$	-364.799 28	-366.748 40	-367.012 29	-367.039 09	-367.050 77	-367.060 04
$SiH_3 + CCH$	-364.812 60	-366.756 21	-367.015 62	-367.046 77	-367.059 04	-367.067 68
$HCCSiH_2 + H$	-364.855 91	-366.798 03	-367.098 87	-367.119 08	-367.127 93	-367.141 64
$[CCH(SiH_3)]^*$ (1,2 silyl)	-364.888 15	-366.852 59	-367.168 44	-367.194 63	-367.202 70	-367.217 16
$[CCH(SiH_3)]^*$ (1,2 hydrogen)	-364.863 52	-366.834 67	-367.152 01	-367.176 74	-367.186 52	-367.200 90
$[C_2H_2 + SiH_2]^*$	-364.823 09	-366.763 18	-367.111 38	-367.131 05	-367.140 02	-367.158 01
$[HCCSiH + H_2]^*$	-364.837 97	-366.781 74	-367.125 09	-367.148 67	-367.157 39	-367.173 28

[a] Total energies in au; 1 au = 627.51 kcal/mol.

Table IV. Relative Energies[a]

reaction system	HF/ 3-21G	HF/ 6-31G*	MP2/ 6-31G*	MP3/ 6-31G*	MP4SDQ/ 6-31G*	MP4SDTQ/ 6-31G*	ZPE/ 3-21G	best theor est MP4SDTQ/ 6-31G* + ZPE
$HC{\equiv}CSiH_3 \rightarrow C_2H_2 + SiH_2$	53.3	61.3	66.5	62.2	61.3	62.7	-9.8	52.9
$HC{\equiv}CSiH_3 \rightarrow [C_2H_2 + SiH_2]^*$	89.2	95.4	79.2	79.9	79.5	77.2	-3.0	74.2
$HC{\equiv}CSiH_3 \rightarrow HCCSiH + H_2$	44.6	58.1	54.3	52.1	51.1	51.5	-5.5	46.0
$HC{\equiv}CSiH_3 \rightarrow [HCCSiH + H_2]^*$	79.8	83.8	70.6	68.8	68.6	67.6	-3.0	64.6
$HC{\equiv}CSiH_3 \rightarrow CCH(SiH_3)$	39.1	35.6	48.0	41.6	41.3	42.7	-1.9	40.8
$HC{\equiv}CSiH_3 \rightarrow [CCH(SiH_3)]^*$ (1,2 silyl)	48.3	39.3	43.4	40.0	40.1	40.1	-1.9	38.2
$HC{\equiv}CSiH_3 \rightarrow [CCH(SiH_3)]^*$ (1,2 hydrogen)	63.8	50.6	53.7	51.2	50.3	50.3	-4.9	45.4
$HC{\equiv}CSiH_3 \rightarrow H + CCSiH_3$	104.1	104.7	141.3	137.6	137.6	138.6	-8.8	129.8
$HC{\equiv}CSiH_3 \rightarrow SiH_3 + CCH$	95.8	99.8	139.3	132.8	130.3	133.9	-6.4	127.5
$HC{\equiv}CSiH_3 \rightarrow HCCSiH_2 + H$	68.6	73.6	87.1	87.4	87.1	87.4	-7.0	80.4

[a] Zero-point energies and relative energies in kilocalories per mole.

this is similar to that observed in the addition of silylene,[26] methylsilylene,[13] ethylsilylene,[11] and vinylsilylene[12] to H_2. The vibrational frequencies for this transition structure are characterized by one imaginary frequency as shown in Table II. The transition vector (normal mode associated with the imaginary frequency) consists mainly of the H_2 stretching mode coupled to H_2 translation and rotation and is compatible with the changes in the geometry that occur during the reaction. Furthermore, the imaginary frequency is quite large ($1727i$ cm^{-1}) and is consistent with a narrow barrier.

The total and relative energies for reaction 7 are given in Tables III and IV. At the MP4/6-3G* level, including zero-point energy correction, the transition state for the 1,1 hydrogen elimination reaction lies 64.6 kcal/mol above the ethynylsilane equilibrium structure. This agrees well with the experimental activation energy (61.2 ± 5.2 kcal/mol) measured in shock-tube studies.[15] The barrier for the reverse process (-7) is quite small relative to the other barriers, 18.6 kcal/mol, and is consistent with experimental studies on methylsilane,[5-7] ethylsilane,[1,4] and vinylsilane.[1,9]

The reaction path for 8, 1,2-elimination of SiH_2, passes through a three-center transition state involving two heavy atoms and a hydrogen. The SiH_3 group must break a SiH bond and form a new CH acetylenic bond, as shown in Figure 1c. For ethynylsilane, the transition state occurs later along the reaction path than for vinylsilane and ethylsilane; this is evident from the CH bond lengths: 1.272, 1.407, and 1.574 Å, respectively, at the HF/6-31G* level. Viewed in the reverse direction, the reaction is the insertion of SiH_2 into the CH bond of acetylene and occurs early along the reaction coordinate. Calculated vibrational frequencies given in Table II for this transition structure reveal that this structure is a true first-order saddle point with one imaginary frequency. Computed barrier height for ethynylsilane dissociation to C_2H_2 and SiH_2 is 74.2 kcal/mol at the MP4/6-31G* with zero-point energy correction. The corresponding barriers for dissociation of ethylsilane to C_2H_6 and SiH_2 and vinylsilane to C_2H_4 and SiH_2 are 72.2 kcal/mol (MP4SDQ/6-31G*)[11] and 68.7 kcal/mol (MP4SDTQ/6-31G*),[12] respectively. Consequently, the calculated barrier for ethynylsilane 1,3-elimination of SiH_2 appears to be reasonable.

(26) Francisco, J. S.; Kurz, C.; McDouall, J. J. W., to be published.

The isomerization reaction of ethynylsilane can take place via two different processes: a 1,2 hydrogen shift via

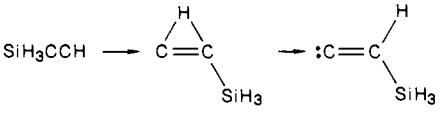

(13)

or 1,2 silyl shift via

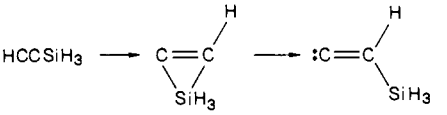

(14)

Both processes have been examined, and the geometries for the transition states are given in Table I. In the transition state for the 1,2 silyl shift, computed at the HF/3-21G level of theory, the SiH_3 group is 0.3 Å closer to the carbon containing the remaining hydrogen than to the other carbon, and the transition structure resembles the final product and is indicative of a late transition state. When polarization functions are added, the transition state shifts significantly toward the product, the $\angle C_1C_2Si$ angle changes from 72.9° (3-21G) to 59.3° (6-31G*).

For the back-reaction (15), there is a 9.2 kcal/mol barrier. At the HF/6-31G* level this barrier decreases to 3.7 kcal/mol and disappears entirely when correlaction is included at the MPn/6-31G* level. To study this process further, we have optimized

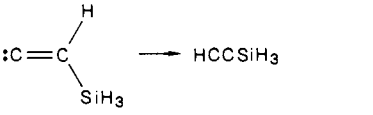

(15)

the geometries of the reactant, the intermediate, and several points along the path connecting the two at the MP2/3-21G* level. We have found no maximum or transition state but rather a smoothly increasing energy profile (i.e. no barrier to the back-reaction). This suggests that silylvinylidene, $:CCH(SiH_3)$ may be a transient species rather than a true intermediate. Nevertheless, it can undergo secondary reactions leading to dissociation. A 1,3 hydrogen shift leading to the elimination of silylene and the production of acetylene via is a good candidate for this secondary process and is consistent with the observation that acetylene is

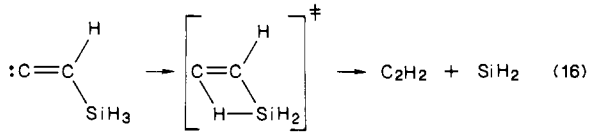

(16)

the major product. Preliminary calculations indicate that reaction 16 takes place via a four-center transition state involving a 1,3 hydrogen shift from the silyl group to the carbon lone pair; this reaction proceeds without a barrier at the HF/3-21G and HF/6-31G* levels. The computed heat of reaction for silylvinylidene dissociation (16) into C_2H_2 and SiH_2 is 18.8 kcal/mol at the MP4SDTQ/6-31G* level of theory (the details of the structure and energetics of this process will be elaborated in a forthcoming paper[26]). Consequently, the dissociation of ethynylsilane to observed products takes place in a two-step process through a transient species, $:CCH(SiH_3)$ during the dissociation process. The net energetics is represented by summing up the heat of reactions 14 and 16, since no activation barriers are involved in either reaction. The net energy of activation is 57.0 kcal/mol for $HC{\equiv}CSiH_3 \rightarrow [:C{=}CH(SiH_3)]^* \rightarrow C_2H_2 + SiH_2$. This compares quite favorably with the activation energy of 61.2 ± 5.2 kcal/mol obtained experimentally for the decomposition. Note that this route is 17.2 kcal/mol lower in energy than the direct 1,2 SiH_2 elimination route (8).

The 1,2 hydrogen shift reaction (13) can also take place and may be an important pathway at higher energies (see below). At the HF/3-21G, HF/6-31G*, and MP4/6-31G* levels this process is energetically less favored than the shift of the silyl group by 12.5, 8.3 and 7.4 kcal/mol, respectively. However, it should be noted that the 1,2 hydrogen shift is significantly lower in energy than the paths that lead to the elimination of molecular hydrogen (18.3 kcal/mol lower at MP4/6-31G* with zero-point correction) or the elimination of silylene (27.9 kcal/mol lower). Hence, the formation of the silylvinylidene by either path is favored over 1,1 H_2 or 1,2 SiH_2 eliminations, reactions 7 and 8, respectively.

Finally, looking at the relative energetics of the fragmentation processes in reactions 10–12, it can be seen that reaction 10 and 11 are high-energy processes compared with isomerization or elimination paths. The fragmentation process represented in (12) is significantly lower in energy than either (10) or (11). At the HF/3-21G level this process is only 3.5 kcal/mol higher in energy than the 1,2 hydrogen shift transition state (13) and may be competitive.

In summary, we have located the transition structures that account for the two elimination reactions proposed by Ring and co-workers.[15,16] The transition structure we have obtained for the direct SiH_2 elimination, reaction 8, is very different from that postulated by Rogers et al.,[15,16] i.e. To investigate this further,

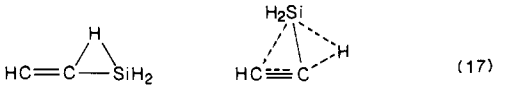

(17)

a geometry resembling the structure proposed by Rogers et al.[15,16] was taken as the starting point for a geometry optimization. The structure was fully optimized, and a frequency calculation showed this structure to be a second-order saddle point; that is to say, the potential energy hypersurface has 2 degrees of freedom with negative curvature. Since a true transition state may have only 1 degree of freedom with negative curvature, the structure proposed in ref 15 cannot be a transition state. One negative eigenvalue, $-302\ cm^{-1}$, corresponded almost solely to the transfer of the silyl group from C_1 to C_2, while the other negative eigenvalue, $-1757\ cm^{-1}$, corresponded to the shift of the migrating hydrogen from Si to C. The energy of the second-order saddle point at the HF/3-21G level of theory is found to be 18 kcal/mol higher in energy than the transition state for the direct 1,2 SiH_2 elimination process (8) (depicted on the left-hand side of (17)). Hence, this gives a barrier of 107.2 kcal/mol. While the addition of correlation to this structure may be expected to reduce this by some 15 kcal/mol (by comparison with Table IV), it cannot be

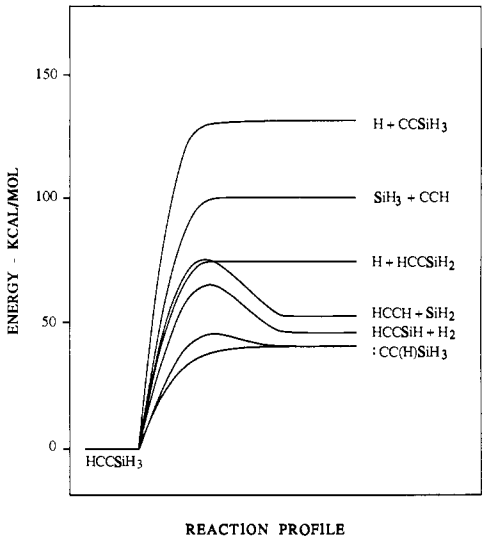

Figure 2. Summary of potential energy curves for primary dissociation pathways for ethynylsilane.

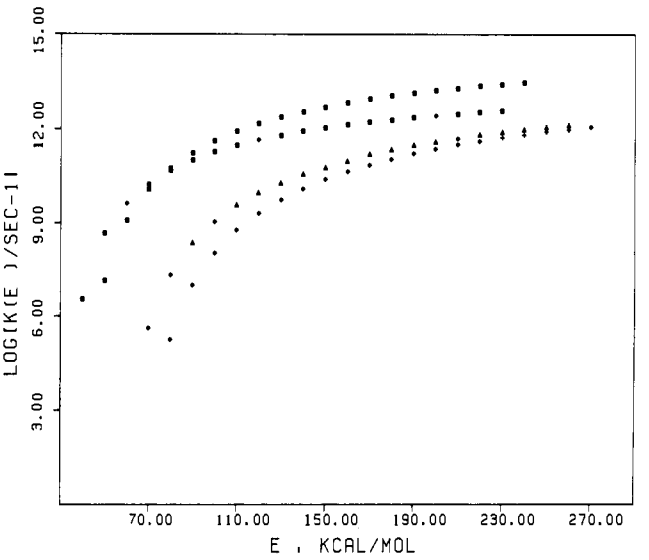

Figure 3. Unimolecular dissociation rates for primary molecular dissociation pathways of ethynylsilane as a function of energy: (●) C_2HSiH_3 (1,2 silyl shift), (■) C_2HSiH_3 (1,2 hydrogen shift), (▲) $C_2HSiH + H_2$, (+) $C_2H_2 + SiH_2$.

expected to overcome the difference in energy between the two structures depicted in (17) or in (9). Consequently, the isomerization leading to the silylvinylidene (reactions 9, 13, or 14 and subsequent SiH_2 elimination (16) may be an energetically important process, which could predominate the primary dissociation process for ethynylsilane. A summary of the potential energy surface for ethylsilane is shown in Figure 2.

To further illustrate the dominance of reaction 14, we have performed RRKM calculations to determine energy-dependent unimolecular dissociation rates, in order to assess the relative importance of primary reactions 7, 8, 13, and 14 kinetically. The input parameters used were the frequencies for the reactant and transition states given in Table II, the reduced internal moments of inertia for the reactant and transition states are calculated from the optimized geometries of the HF/6-31G* level of theory, and the critical energies for each pathway given in Table IV were obtained at the MP4/6-31G*//HF/6-31G* level. Our results are summarized in Figure 3. The salient point of these calculations is that the three-centered silyl shift mechanism (reaction 14) is seen to be a fast process at relatively low molecular energies. Consequently, in the low-energy range this process dominates, while at higher energies the 1,2 hydrogen shift mechanism (reaction 13) dominates. This behavior can be attributed to the fact

that, at higher molecular energies, the density of higher energy states accessed in the hydrogen shift process prevails over the silyl shift process. We also note that reactions 13 and 14 predominate the dissociation over all energies; rates for this process are estimated to be 2–4 orders of magnitude faster than that for the 1,1 H_2 elimination (reaction 7) and 1,2 SiH_2 elimination (reaction 8). Taking the rate into account, the dominant pathway for decomposition is expected to be isomerization of ethynylsilane via reaction 9 followed by elimination of SiH_2 via reaction 16.

Conclusion

Primary dissociation pathways of ethynylsilane have been examined, and we find that pathways leading to the newly postulated species silylvinylidene, :CCH(SiH_3), are preferred energetically and kinetically. Silylvinylidene is suggested to be a transient species, which proceeds to dissociation, without barrier, to the products C_2H_2 and SiH_2. The net activation energy for the process is calculated to be 57.0 kcal/mol at the MP4SDTQ/6-31G* level of theory and is in good agreement with experiment. Other pathways leading to the observed products have been discounted. We note that C_2H_4 is a minor product of the decomposition studies of ethynylsilane.[1] No primary dissociation pathways of reasonable energy leading to C_2H_4 could be found. Consequently, we conclude that C_2H_4 results from secondary reactions.

Acknowledgment. We are grateful to Wayne State University Computer Center and Chemistry Department for provision of computing resources, the National Science Foundation for a Presidential Young Investigator Award (J.S.F.), and the NSF for Grant CHE-87-11901 (H.B.S.).

Tetrazetidine: Ab Initio Calculations and Experimental Approach

G. Ritter,[†,‡] G. Häfelinger,*[,†] E. Lüddecke,[§,⊥] and H. Rau*[,§]

Contribution from the Institut für Organische Chemie, Universität Tübingen, 7400 Tübingen, West Germany, and FG Physikalische Chemie, Institut für Chemie, Universität Hohenheim, 7000 Stuttgart 70, West Germany. *Received July 13, 1988*

Abstract: The kinetic analysis of the photoreaction system of azobenzenophanes is presented. We find, besides the cis and trans forms, a transient species living for a few minutes. All experimental evidence we have is compatible with a tetrazetidine structure of this species. The molecular structures of five configurational isomers of the hitherto unknown parent tetrazetidine have been calculated by ab initio restricted Hartree–Fock self-consistent field molecular orbital gradient optimizations using STO-3G, 6-31G, and 6-31G** basis sets. Geometries and total energies of the isomers with nonplanar, quadratic, and rectangular arrangements of the ring nitrogens are reported. The formation of tetrazetidine by approach to two *trans*-diazene molecules was simulated with optimization at all intermolecular separations R for a parallel [$\pi^2s + \pi^2s$] ground-state reaction pathway. Although all isomers of tetrazetidine are energetically less stable than their diazene dissociation products, the tetrazetidine seems to be trapped kinetically by rather high energy barriers.

1. Introduction

The four-membered ring system built only of nitrogen atoms is one of the few simple structures in organic chemistry that has not yet been synthesized. Indeed, a search for tetrazetidine in CAS-Online produces only the registry no. 58674-00-3 and two references which, however, do not mention the structure.

In the course of our investigations of the thermal and photoisomerization of the azobenzenophane **1**,[1] we realize some peculiarities that find an easy explanation if the formation of a tetrazetidine species **2** is assumed.

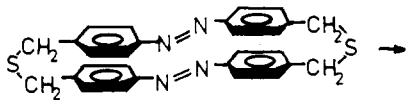

1

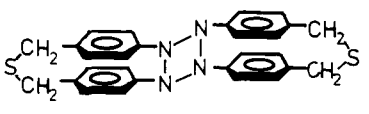

2

As the experimental evidence for the formation of a tetrazetidine structure is still indirect, we have tried to gain firm ground by employing ab initio restricted Hartree–Fock SCF MO calculations with analytical gradient optimization of possible molecular structure using STO-3G, 6-31G, and 6-31G** basis sets. Of course we had to restrict ourselves to the parent tetrazetidine system. These calculations are the first ones for tetrazetidine, and they give a result surprising for the organic chemist in that tetrazetidine should be a kinetically stable molecule accessible in a photoreaction.

2. Theoretical Approach to Tetrazetidine Formation

1. Ab Initio Calculations of the Molecular Structures and Stabilities for the Ground State of Configurational Isomers of Tetrazetidine. To the best of our knowledge no ab initio calculations of the molecular system of tetrazetidine are reported in the literature. There are, however, many calculations known for hydrazine[2-4] (**8**) and *trans*- and *cis*-diazene[4-9] (**9**, **10**) which are

[†] Universität Tübingen.
[‡] Present address: Wella AG, Darmstadt, West Germany.
[§] Universität Hohenheim.
[⊥] Present address: BASF AG, Ludwigshafen, West Germany.

(1) Rau, H.; Lüddecke, E. *J. Am. Chem. Soc.* **1982**, *104*, 1616.
(2) Pasto, D. J. *J. Am. Chem. Soc.* **1979**, *101*, 6852–6857.
(3) Tanaka, N.; Hamada, Y.; Sugawara, Y.; Tsuboi, M. Kato, S., Morokuma, K. *J. Mol. Spectrosc.* **1983**, *99*, 245–262.
(4) Whiteside, A.; Binkley, J. S.; Krishnan, R.; DeFrees, D. J.; Schlegel, H. B.; Pople, A. J.: Carnegie-Mellon Quantum Chemistry Archive, Pittsburgh, 1980.
(5) Jensen, A. J. A.; Jorgensen, P.; Helgaker, T. *J. Am. Chem. Soc.* **1987**, *109*, 2895–2901.
(6) Winter, N. W.; Pitzer, R. M. *J. Chem. Phys.* **1975**, *62*, 1269–1275.
(7) Binkley, J. S.; Pople, J. A.; Hehre, W. J. *J. Am. Chem. Soc.* **1980**, *102*, 939–947.
(8) Pouchan, C.; Dargelos, A.; Chaillet, M. *J. Mol. Spectrosc.* **1979**, *76*, 118–130.

0002-7863/89/1511-4627$01.50/0